

PAPER

# Evolution of magnetic surfboards and spin glass behavior in $(\text{Fe}_{1-p}\text{Ga}_p)_2\text{TiO}_5$

To cite this article: Y Li *et al* 2023 *J. Phys.: Condens. Matter* **35** 475401

View the [article online](#) for updates and enhancements.

## You may also like

- [Structure and energetics of FeO/Fe\(001\) interfaces](#)  
Tomasz Ossowski and Adam Kiejna
- [Antiferromagnetic order and its interplay with superconductivity in  \$\text{CaK}\(\text{Fe}\_{1-x}\text{Mn}\_x\)\text{As}\_4\$](#)   
J M Wilde, A Sapkota, Q-P Ding et al.
- [Coulomb staircase in an asymmetrically coupled quantum dot](#)  
G McArdle, R Davies, I V Lerner et al.

# Evolution of magnetic surfboards and spin glass behavior in $(\text{Fe}_{1-p}\text{Ga}_p)_2\text{TiO}_5$

Y Li<sup>1,\*</sup> , D Phelan<sup>1,\*</sup> , F Ye<sup>2</sup>, H Zheng<sup>1</sup>, E Krivyakina<sup>1,3</sup>, A Samarakoon<sup>1</sup>, P G LaBarre<sup>4</sup> , J Neu<sup>5,6</sup>, T Siegrist<sup>5,7</sup>, S Rosenkranz<sup>1</sup>, S V Syzranov<sup>4</sup> and A P Ramirez<sup>4,\*</sup>

<sup>1</sup> Materials Science Division, Argonne National Laboratory, Lemont, IL 60439, United States of America

<sup>2</sup> Neutron Scattering Division, Oak Ridge National Laboratory, Oak Ridge, TN 37830, United States of America

<sup>3</sup> Department of Physics, Northern Illinois University, DeKalb, IL 60115, United States of America

<sup>4</sup> Physics Department, University of California Santa Cruz, Santa Cruz, CA 95064, United States of America

<sup>5</sup> National High Magnetic Field Laboratory, Tallahassee, FL 32310, United States of America

<sup>6</sup> Nuclear Nonproliferation Division, Oak Ridge National Laboratory, Oak Ridge, TN 37831, United States of America

<sup>7</sup> Department of Chemical and Biomedical Engineering, FAMU-FSU College of Engineering, Tallahassee, FL 32310, United States of America

E-mail: [yu.li@anl.gov](mailto:yu.li@anl.gov), [dphelan@anl.gov](mailto:dphelan@anl.gov) and [apr@ucsc.edu](mailto:apr@ucsc.edu)

Received 26 April 2023, revised 18 July 2023

Accepted for publication 9 August 2023

Published 29 August 2023



CrossMark

## Abstract

The unusual anisotropy of the spin glass (SG) transition in the pseudobrookite system  $\text{Fe}_2\text{TiO}_5$  has been interpreted as arising from an induced, van der Waals-like, interaction among magnetic clusters. Here we present susceptibility ( $\chi$ ) and specific heat data ( $C$ ) for  $\text{Fe}_2\text{TiO}_5$  diluted with non-magnetic Ga,  $(\text{Fe}_{1-p}\text{Ga}_p)_2\text{TiO}_5$ , for disorder parameter  $p = 0, 0.11$ , and  $0.42$ , and elastic neutron scattering data for  $p = 0.20$ . A uniform suppression of  $T_g$  is observed upon increasing  $p$ , along with a value of  $\chi(T_g)$  that increases as  $T_g$  decreases, i.e.  $d\chi(T_g)/dT_g < 0$ . We also observe  $C(T) \propto T^2$  in the low temperature limit. The observed behavior places  $(\text{Fe}_{1-p}\text{Ga}_p)_2\text{TiO}_5$  in the category of a strongly geometrically frustrated SG.

Keywords: anisotropic spin glasses, neutron scattering, geometric frustration

(Some figures may appear in colour only in the online journal)

## 1. Introduction

The pseudobrookite compound  $\text{Fe}_2\text{TiO}_5$  is unusual for exhibiting spin glass (SG) freezing signatures—a cusp in susceptibility,  $\chi(T)$ , at the glass transition temperature,  $T_g$ , and hysteresis in  $\chi(T)$  below  $T_g$ —only with the applied magnetic field along the crystallographic  $c$ -axis [1]. When probed in the  $a$  and  $b$  directions, no anomaly is seen at  $T_g$ , which is highly unusual because the magnetic ion,  $\text{Fe}^{3+}$ , is an  $s$ -state ion and thus possesses no single-ion anisotropy. In addition, the Fe and Ti atoms randomly occupy the two cation sites.

When a similar  $s$ -state ion,  $\text{Mn}^{2+}$ , resides on a periodic lattice, such as in  $\text{MnF}_2$ , anisotropy develops below the Néel transition due to the dipole–dipole energy, which establishes an ordering direction. It seems unlikely, therefore, given the randomness of the  $\text{Fe}^{3+}$  ions, that this mechanism can explain the anisotropy in  $\text{Fe}_2\text{TiO}_5$ . Thus, it is also likely impossible to describe the complete anisotropy in its SG response using atomic spins as the freezing degree of freedom. Recently we revisited this problem and showed, using neutron scattering, that the Fe spins develop nano-sized regions of antiferromagnetic (AF) order where the spins are either aligned or anti-aligned with the long direction, parallel to the  $a$ -axis [2]. These regions take the shape of surfboards with correlations lengths

\* Authors to whom any correspondence should be addressed.

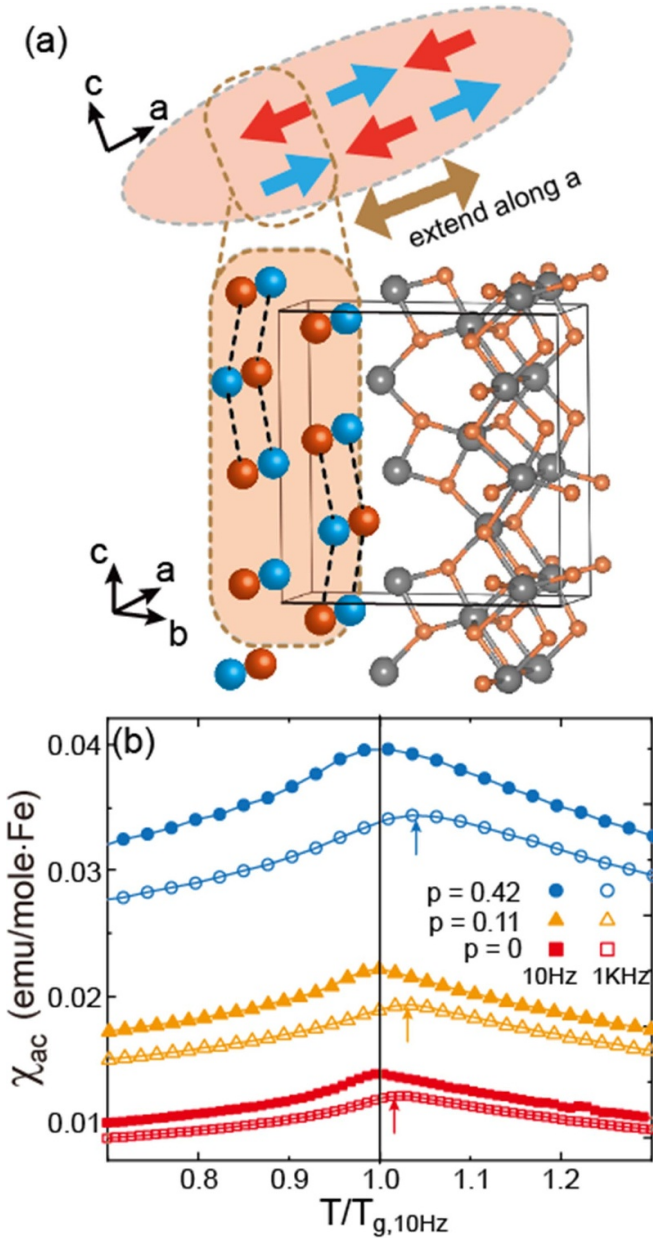


**Figure 1.** Illustration of the crystal and magnetic structure in  $\text{Fe}_2\text{TiO}_5$ . The Fe/Ti positions are represented by large spheres and the oxygen atoms by small yellow spheres. The large spheres are colored red (blue), indicating spins that are parallel (anti-parallel) with the  $a$ -axis, respectively. The grey color indicates that the direction of the spins is undetermined due to geometric frustration. The oxygen atoms on the left part of the unit cell are omitted to better show the double corrugated spin chains as indicated by the dashed lines. The shaded area represents a cross-section of the mesoscopic surfboard (top) that extends along the  $a$ -axis, as determined in [2]. (b) Magnetic ac susceptibility along the  $c$ -axis were measured on  $(\text{Fe}_{1-p}\text{Ga}_p)_2\text{TiO}_5$  compounds with  $p = 0, 0.11$  and  $0.42$ . A modest shift in  $T_g$  as expected for a spin glass is clearly seen to higher temperature with increasing frequency.

of  $\text{\AA} \times 10 \text{\AA}$  along the  $a$ - and  $c$ -axis, respectively, but along the  $b$ -axis, only nearest neighbor spins are correlated due to frustration (figure 1). The principal building block of these surfboards are corrugated AF chains, as depicted in figure 1(a). The frustrated coupling between such chains leads to the

short-range order within surfboards. We also showed that the interaction between the surfboards comes from the fluctuations of their magnetization along the  $c$ -direction, i.e. the direction transverse to the ordered spins. Such a *magnetic van der Waals* force can thus explain, at least qualitatively, the anisotropy of freezing in  $\text{Fe}_2\text{TiO}_5$ .

An important aspect of  $\text{Fe}_2\text{TiO}_5$  is its strong geometrical frustration, as indicated by a large frustration parameter,  $f \equiv \theta_W/T_g = 900/55 \approx 16$  [3], where  $\theta_W$  is the Curie–Weiss temperature. As described in recent work by two of us [4], when varying the amount of quenched disorder in strongly geometrically frustrated (GF) systems, the SG transition temperature  $T_g$  and magnetic susceptibility  $\chi(T_g)$  follow the universal trend  $d\chi(T_g)/dT_g < 0$ , which is opposite to the trend  $d\chi(T_g)/dT_g > 0$  displayed by conventional SGs. Furthermore,  $T_g$  in strongly GF materials grows with decreasing the density of vacancies [4], the dominant source of quenched disorder. This trend calls into question the achievability of quantum spin liquids widely sought in these materials, because it suggests that the SG state, believed to be incompatible with quantum spin liquids, occurs even in very clean samples.

Although  $\text{Fe}_2\text{TiO}_5$  belongs to the same class of strongly GF materials, it is distinct from other GF materials in that it develops the described surfboard-shaped clusters and these clusters apparently play an essential role in the SG freezing. The strong interaction between these clusters, in addition to the strong super-exchange interaction between  $\text{Fe}^{3+}$  spins, may be responsible, for example, for higher SG-transition temperatures in  $\text{Fe}_2\text{TiO}_5$  than in the other GF systems [4]. The SG transition and the structure of the glass state in  $\text{Fe}_2\text{TiO}_5$  thus require a separate careful investigation.

Here, we present  $\chi(T)$  and specific heat ( $C(T)$ ) results for the dilution series  $(\text{Fe}_{1-p}\text{Ga}_p)_2\text{TiO}_5$  for  $0 \leq p \leq 0.42$ , in which non-magnetic  $\text{Ga}^{3+}$  substitutes for  $\text{Fe}^{3+}$ , as well as neutron scattering data for  $p_{\text{nominal}} = 0.20$ . Similar to other GF systems where  $f \gtrsim 10$ , we find that  $T_g$  decreases with increasing susceptibility,  $d\chi(T_g)/dT_g < 0$ , as disorder is increased with Ga content,  $p$ . The specific heat also displays a low-temperature quadratic-in- $T$  term that grows with  $p$ , similar to that seen in other GF materials. Our neutron scattering measurements indicate the existence of surfboard-shaped correlated regions, like in  $\text{Fe}_2\text{TiO}_5$ , but substantially shrinking, as  $p$  is increased. Thus, whereas  $T_g$  reduction in other GF systems is due to an increase in vacancies around which ‘quasispins’ form and undergo freezing, in  $(\text{Fe}_{1-p}\text{Ga}_p)_2\text{TiO}_5$  the quasispins are AF-ordered surfboard-shaped regions. This distinction, in addition to the large exchange coupling reflected by the  $\theta_W$ , may explain why the energy scale for SG freezing is larger in the present material than in other GF systems. Nevertheless, in both types of systems the quasispin is a composite object, i.e. formed from many atomic spins and, thus noted, the argument of [4] pertains.

## 2. Methods

In the present study, we used crystals of  $(\text{Fe}_{1-p}\text{Ga}_p)_2\text{TiO}_5$ , grown by J P Remeika [5] for measurements of magnetic

susceptibility and specific heat. Because these crystals were grown from a flux, their nominal concentrations serve only as a coarse guide to the resultant concentrations. Also, since techniques for atom identification in the solid state, such as energy dispersive atomic spectroscopy, possess systematic uncertainty in ratios between constituent atoms, we rely here on the susceptibility itself to determine the concentration of Fe in each sample. This approach relies on our previously reported measurement of  $\chi(T)$  in  $\text{Fe}_2\text{TiO}_5$  for temperatures between 400 K and 900 K, which yielded an effective moment of  $\mu_{\text{eff}} = 6.12 \pm 0.05 \mu_B$ , in reasonable agreement with the value  $\mu_{\text{eff}} = 5.92 \mu_B$  expected for a free  $S = 5/2$  ion [2]. Since the most concentrated compound of the series yielded an effective moment close to the theoretical value, it is reasonable to expect that the effective moment in more dilute compounds will be identical since the chemical environment and oxidation states are the same. We note that, since  $\text{Fe}^{3+}$  and  $\text{Ti}^{4+}$  can each occupy either the A or B sites in the pseudobrookite  $\text{A}_2\text{BO}_5$  structure, even for  $p = 0$ , the Fe occupation is random. In addition, due to the different oxidation states of Fe and Ti, the pure pseudobrookite compound,  $\text{Fe}_3\text{O}_5$ , cannot be made with only trivalent Fe ions, i.e. with zero magnetic disorder. Since  $\text{Ga}^{3+}$  is isovalent with  $\text{Fe}^{3+}$  but non-magnetic and similar in size, substituting it for  $\text{Fe}^{3+}$  will increase magnetic disorder while decreasing spin density. We studied flux-grown crystals for 3 nominal values:  $p_{\text{nominal}} = 0, 0.3, \text{ and } 0.5$ . Based on the effective moment from high temperature susceptibility, we estimated the corresponding actual concentrations to be  $p_{\text{estimate}} = 0, 0.11, \text{ and } 0.42$ ; hereafter, we refer to the values of  $p$  by those determined via  $p_{\text{estimate}}$  for simplicity. A larger single crystal with  $p_{\text{nominal}} = 0.2$  for neutron scattering was grown at Argonne National Laboratory in a floating zone furnace. Based on comparison of  $T_g$  measured by magnetometry of a single crystal fragment grown by the floating zone to those measured for the flux-grown crystals, we estimated the concentration to be  $p_{\text{estimate}} = 0.17$ . Structural refinements of full single-crystal x-ray diffraction datasets, collected using an Oxford Diffraction Xcalibur-2CCD diffractometer indicated almost complete random occupation of the A and B-sites in the pseudobrookite-type structure by Ti, Fe, and Ga, with a slightly higher electron count, of the order of 0.8 electrons or an average of 26 electrons on the B-site. This thus suggests that the increasing magnetic disorder on both A and B-sites with increasing  $p$  is notionally correct.

### 3. Results

The crystal structure of the flux-grown crystals was confirmed by single crystal x-ray diffraction to be the pseudobrookite phase. The orthorhombic lattice constants  $\{a, b, c\}$  in Ångstroms for  $p = 0, 0.11, \text{ and } 0.42$  are  $\{3.732(1), 9.8125(2), 10.0744(2)\}$ ,  $\{3.7023(1), 9.7872(2), 9.9670(2)\}$  and  $\{3.6857(1), 9.7903(2), 9.9681(2)\}$  respectively. The dependence of  $\{a, b, c\}$ , as well as the volume of the unit cell  $V(p)$ , on  $p$  is shown in the upper left inset of figure 2, normalized to their  $p = 0$  values. The volume monotonically decreases with increasing  $p$ , consistent with the smaller

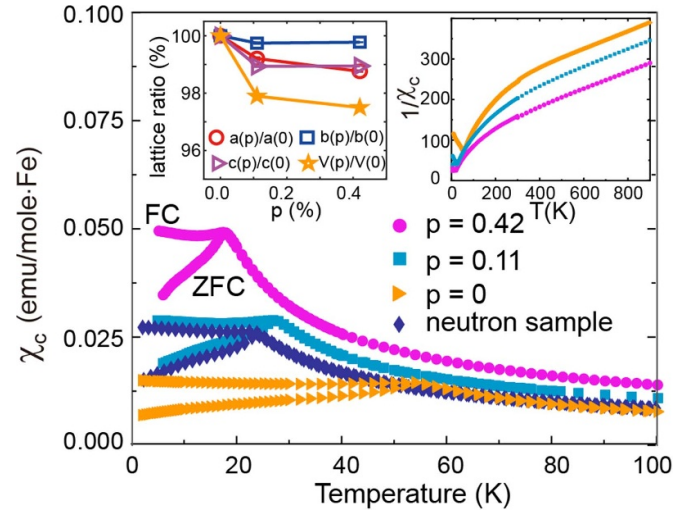


**Figure 2.**  $C$ -axis susceptibility of  $(\text{Fe}_{1-p}\text{Ga}_p)_2\text{TiO}_5$  for various values of  $p$  measured with an applied field of  $\mu_0H = 0.01$  T. The lower curve at temperatures below each kink were taken after zero field cooling and the upper curves after field cooling. Inset: left, the dependence of lattice constants and the unit cell volume on  $p$ ; right, the inverse susceptibility for the same samples. The  $p$ -values for the samples other than  $p = 0$  were determined by adjusting the molar mass to yield the same high-temperature slope of  $1/\chi(T)$  as the  $p = 0$  sample, the Fe concentration of which is known exactly. The crystal labeled ‘neutron sample’ was a measurement of a small single crystal grown in the same floating zone furnace with the same nominal composition as that as the crystal measured by neutron diffraction.

ionic radius of  $\text{Ga}^{3+}$  compared to  $\text{Fe}^{3+}$  and indicative of successful substitution. The monotonic  $V(p)$  emanates primarily from the monotonic decrease in  $a$  with  $p$ , while there are less changes in  $b$  and  $c$  from  $p = 0.11$  to  $0.42$ . Magnetization measurements were performed in two different Quantum Design Magnetic Property Measurement Systems (MPMS3s). For  $\chi(T < 300$  K), a conventional sample holder was used. For  $\chi(T > 300$  K), the sample was mounted with Zircar cement on a rod designed for high-temperature measurements. The specific heat,  $C(T)$ , was measured for  $T > 2.5$  K using the relaxation technique in a Quantum Design Physical Property Measurement System (PPMS). For  $T < 4$  K,  $C(T)$  was measured using the semi-adiabatic technique in a top-loading dilution refrigerator. Energy dispersive x-ray absorption spectroscopy was performed on the samples and yielded a Fe:Ga ratio that confirmed the general trend expected for Ga substitution. The neutron scattering measurements were performed on the time-of-flight instrument Corelli (ORNL) using a pseudo-white beam [6]. This is the same instrument which was used to measure  $\text{Fe}_2\text{TiO}_5$ , as reported previously [2].

In figure 2 are shown magnetic susceptibility with applied field along the  $c$ -axis,  $\chi_c(T)$ , characterizing the anisotropic SG transition in  $(\text{Fe}_{1-p}\text{Ga}_p)_2\text{TiO}_5$  with  $p = 0, 0.11, \text{ and } 0.42$ . It is important to recognize that, since Fe, Ga, and Ti can each occupy either of the two cation sites, the magnetic ion stoichiometry  $p = 0, 0.11, \text{ and } 0.42$  corresponds to Fe occupancies of  $n_{\text{Fe}} = 0.67, 0.59, \text{ and } 0.39$ . We see that  $T_g$  decreases with decreasing concentration of magnetic ions— $T_g = 55$  K,

27 K, and 18 K, for  $p = 0, 0.11, \text{ and } 0.42$  respectively. While a decrease in  $T_g$  with decreasing concentration of magnetic ions is also seen in conventional SG systems such as  $\text{CuMn}$  [7],  $\text{AuFe}$  [8, 9], and  $\text{Eu}_x\text{Sr}_{1-x}\text{S}$  [10], the increase of  $\chi(T_g)$  with decreasing  $T_g$ ,  $d\chi(T_g)/dT_g < 0$ , is accounted as an effect of vacancy defects on GF magnets [11]. We note here that although the nature of short-range order in the present system, and GF materials in general, is not fully understood, Syzranov has provided a mechanism for the observed behavior of  $\chi(T_g)$  with dilution in the [11]. As discussed in [4], such behavior is, however, a distinct signature of the SG transition in all other GF for which  $f \geq 10$ . The inset of figure 2 shows the inverse susceptibility for the same compounds where, as previously indicated, the  $p = 0.11$  and  $0.42$  data have been scaled to exhibit the same slope and thus the same  $\mu_{\text{eff}}$  as the  $p = 0$  data. To further confirm the SG behavior in doped compounds, we compare the temperature dependent AC susceptibility of  $p = 0, 0.11, \text{ and } 0.42$  around the normalized spin-glass freezing temperatures (i.e.  $T/T_g$ ) in figure 1(b). All three samples have a shift in  $T_g$  to higher temperature with increasing frequency, consistent with behavior in conventional SGs. Indeed, we observed an increasing frequency dispersion (i.e. a larger shift in the normalized  $T_g$ ) as the value of  $p$  was increased. Previous work on the AC susceptibility of  $\text{Fe}_2\text{TiO}_5$  indicated that the frequency dependence of  $T_g$  follows a Vogel–Fulcher law [12, 13].

In figure 3 are shown specific heat data for  $p = 0, 0.11, \text{ and } 0.42$  over different temperature ranges. In figure 3(a),  $C(T)/T$  versus  $T$  up to 300 K is plotted per ‘mole-formula unit’, appropriate for comparing the main contributions, namely lattice and magnetic excitations. These data show a broad hump centered at approximately 140 K, the high-temperature decrease of which indicates an approach on warming into the Dulong–Petit region. The data in this frame are mainly due to lattice excitations, as can be judged from the area of the shaded region which is equal to the total magnetic entropy for  $p = 0$  and approximately 10% of the total entropy from  $T = 0$ –300 K. As the Fe concentration decreases, one can see the height of the broad peak decrease slightly while the entropy below 50 K increases. This entropy shift may be indicating that, as Fe site-occupancy decreases, a greater fraction of spins find themselves in the low-energy region of the rough energy landscape associated with random freezing. In figure 3(b) are shown data at intermediate temperatures. Here, the differences among the data sets reflect the entropy transfer mentioned above. Finally, in figure 3(c) are shown  $C(T)/T$  for  $T$  down to 200 mK, below which an additional, possibly nuclear, contribution appears as a rise in  $C(T)/T$  on decreasing  $T$  for the last few points, especially noticeable for  $p = 0.42$ . Taking this contribution into account, the data are consistent with a linear term that is too small to be unambiguously identified. More apparent is a temperature dependence below  $T = 3\text{ K}$  that is consistent with  $C(T) \propto T^2$ , behavior which has been seen in several other strongly GF systems [14–17]. While the precise origin of the  $C(T) \propto T^2$  behavior is not well understood [17], it is reasonable to ascribe the associated excitations to inter-surfboard spins, and not to intra-surfboard spin waves, since these are

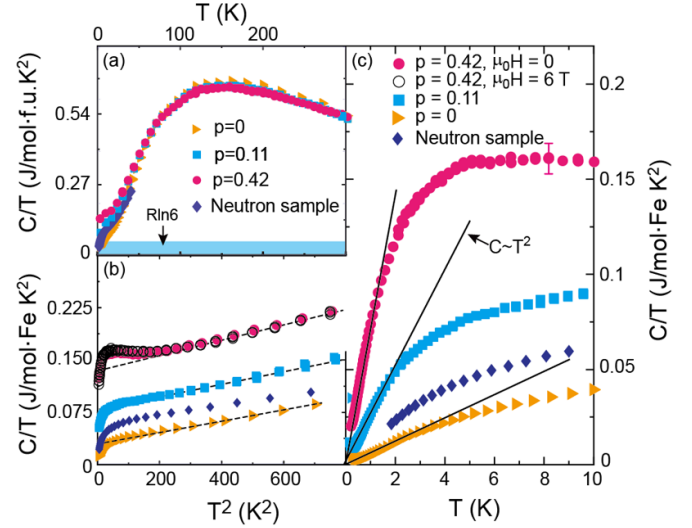


**Figure 3.** Specific heat divided by temperature of  $(\text{Fe}_{1-p}\text{Ga}_p)_2\text{TiO}_5$  for various values of  $p$ . (a)  $(T)/T$  vs. temperature for  $p = 0, 0.11, \text{ and } 0.42$ , each showing a broad maximum at  $T \approx 140$  K, which results from a dominantly phonon contribution to  $C(T)$ . The low temperature shoulder is a consequence of a magnetic contribution. (b)  $(T)/T$  vs  $T^2$  in the intermediate temperature regime shows a crossover from magnetically dominated region (low  $T$ ) to the phonon dominated region where  $C(T) \propto T^3$  expected for phonons. (c)  $(T)/T$  vs  $T$  for  $T < 10$  K, showing that for each composition  $C(T) \propto T^2$  for  $T < 3$  K. The crystal labeled ‘neutron sample’ was a measurement of a small single crystal grown in the same floating zone furnace with the same nominal composition as that as the crystal measured by neutron diffraction.

expected to follow  $C(T) \propto T^3$ , albeit with a strong finite-size effect, which should produce a gap in the spin wave spectrum. In general, the specific heat of a disordered spin system may come from itinerant spin modes, such as Halperin–Saslow [18, 19] modes or spin–lattice ‘photons’ [20–24], or from localized excitations [19]. Such itinerant modes can result in the  $C(T) \propto T^2$  in an effectively 2D, e.g. layered, system. In 3D, however, they will lead to the  $C(T) \propto T^3$  temperature dependence, inconsistent with our observations here.

It is reasonable, therefore, to ascribe the observed quadratic specific heat to localized excitations among inter-surfboard spins. The quadratic dependence of the specific heat requires that the density of states (DoS) of these excitations (the density of levels per unit energy in an ensemble of excitations),  $\nu(E)$ , be linear in energy  $E$ . As shown in [25], in a strongly disordered medium with short-range interactions, a linear-in- $E$  DoS is a universal feature of excitations corresponding to shifting any conserved quantity between nearby sites (quasi-localized states). The role of such a quantity may be played by spin density or ‘charge’ in the Coulomb phase [20, 21, 26–28] of a GF magnet. The corresponding mechanism requires that the shifts of the conserved quantity do not become arbitrarily large (which is possible in metastable states such as SGs). Because the DoS of excitations is field-independent in strongly disordered systems, the respective contribution to the specific heat will be field-independent, as is observed between  $H = 0$

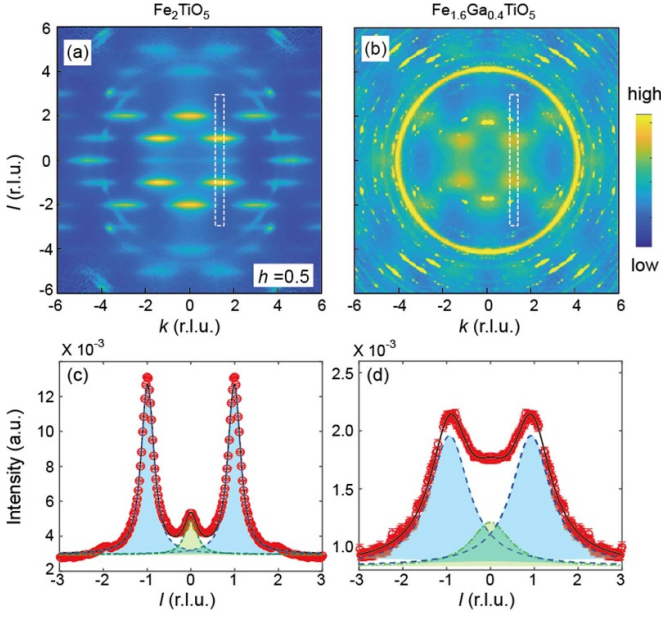


**Figure 4.** Total neutron scattering intensity in the  $[0.5, k, l]$  planes for  $\text{Fe}_2\text{TiO}_5$  at  $T = 5$  K (a) and  $\text{Fe}_{1.6}\text{Ga}_{0.4}\text{TiO}_5$  ( $p = 0.20$ ) at  $T = 6$  K (b). (c) and (d) Total neutron scattering intensity along the  $l$ -direction as indicated by the dashed rectangle in (a) and (b), respectively. The intensity was fitted with three Lorentz functions convoluted with a Gaussian resolution function. The three Lorentz peaks are set to have the same HWHM whose reversal is the correlation length along the  $l$ -direction and is estimated to be  $3.0 \pm 0.1$  Å at 6 K and  $2.7 \pm 0.1$  Å at 50 K for  $\text{Fe}_{1.6}\text{Ga}_{0.4}\text{TiO}_5$  and  $10.9 \pm 0.15$  Å at 5 K and  $9.6 \pm 0.15$  Å at 60 K for  $\text{Fe}_2\text{TiO}_5$ .

and 6 T for the  $p = 0.42$  compound, shown in figure 3(c). We leave, however, an investigation of the exact nature of the corresponding excitations for future studies.

Despite similarities with other GF systems, an important distinction can be drawn since, in  $(\text{Fe}_{1-p}\text{Ga}_p)_2\text{TiO}_5$ , the degrees of freedom that undergo SG freezing are postulated to be the surfboard-shaped ordered regions seen in neutron scattering [2]. The size of these regions in the undoped limit ( $p = 0$ ) is approximately  $40$  Å  $\times$   $3$  Å  $\times$   $10$  Å, and thus an order of magnitude larger in the  $a$ -direction than the size of typical vacancy-induced quasi-spins which are thought to undergo freezing in other GF systems [29, 30]. Indeed, the large surfboard size, coupled with the observation that the ordered intra-surfboard spins point along the  $a$ -axis, whereas spin freezing is seen only along the  $c$ -axis, suggested a surfboard-surfboard interaction induced by fluctuations in the magnetization that are transverse to the spin ordering direction in the surfboards [2]. Below we describe the evolution of surfboard size and shape with  $\text{Fe}^{3+}$  dilution.

Comparison of the magnetic diffuse neutron diffraction patterns of the  $p = 0$  and  $p = 0.20$  is shown in figures 4 and 5. Figures 4(a) and (b) contrast the data measured in the  $(1/2, k, l)$  plane for these two compositions. The peaks in scattering intensity are highly elliptical for  $p = 0$ , being broad along  $k$  and sharper along  $l$ , which reflects the differing correlation lengths along these two directions. Correlations along  $b$  are limited to

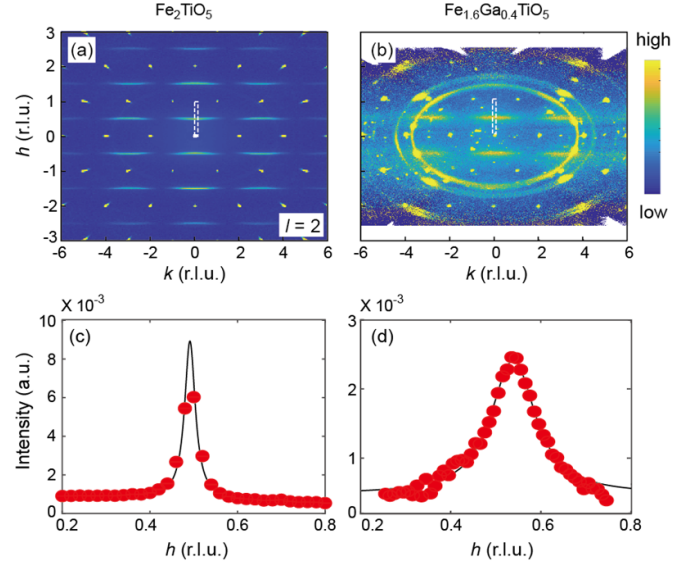


**Figure 5.** Total neutron scattering intensity in the  $(h, k, 2)$  planes for  $\text{Fe}_2\text{TiO}_5$  at  $T = 5$  K (a) and  $\text{Fe}_{1.6}\text{Ga}_{0.4}\text{TiO}_5$  at  $T = 6$  K (b). (c) and (d) Total neutron scattering intensity along the  $h$ -direction as indicated by the dashed rectangle in (a) and (b), respectively. The intensity was fitted with single Lorentzian functions convoluted with a Gaussian resolution function. The correlation length along the  $h$ -direction is estimated to be  $10.8 \pm 0.7$  Å at 5 K and  $7.5 \pm 0.6$  Å at 50 K for  $\text{Fe}_{1.6}\text{Ga}_{0.4}\text{TiO}_5$  and  $40.5 \pm 1.0$  Å at 5 K and  $32.1 \pm 0.9$  Å at 60 K for  $\text{Fe}_2\text{TiO}_5$ .

nearest neighbors; however, along  $c$  the correlation length is about 11 Å as determined from the inverse of the half-width-half maximum of Lorentzian fits of a cut through the peaks along  $l$  as shown in figure 4(c). These results are consistent with our previous results for  $p = 0$  [2]. For  $p = 0.20$ , the peaks occur at the same positions in reciprocal space as for  $p = 0$ , indicating the continued presence of surfboard-shaped correlation regions for smaller Fe site occupancy. The peak widths along  $k$  indicate that the correlations are similarly nearest neighbor-limited along  $b$ . However, the peaks are significantly broader along  $l$  for  $p = 0.20$  than for  $p = 0$ , and the Lorentzian fits shown in figure 4(d) indicate that the correlation length is significantly reduced at  $T = 5$  K to only  $\sim 3$  Å, approaching the correlation length along  $b$ . Further, it is quite apparent that the peaks in the  $(h, k, 2)$  planes (figures 5(a) and (b)) are broader for  $p = 0.20$  than for  $p = 0$ . Fits along  $h$  indicate that, despite considerable reduction induced by Ga dopants, the correlation length along  $a$  for  $p = 0.20$  at 5 K remains significantly longer than the lattice constant, with a value of  $\sim 11$  Å, resulting in regions with a size  $\sim 11$  Å  $\times$   $3$  Å  $\times$   $3$  Å. Thus, while the aspect ratio of the correlated regions remains surfboard-like, the shape has become more prolate than for  $p = 0$ .

## 4. Discussion

The decrease in surfboard size (magnetic correlation length) with increasing  $p$  is consistent with the associated decrease

in  $T_g$ : smaller surfboard sizes correspond to smaller fluctuations of the magnetization on the surfboard, weaker interactions between the surfboards and, concomitantly, lower glass transition temperature  $T_g$  (in accordance with the quantitative description developed in [2] for the  $p = 0$  case). Increasing the density of  $\text{Ga}^{3+}$  ions, or non-magnetic vacancies, leads to the existence of fewer regions of large-enough  $\text{Fe}^{3+}$  density to support the surfboard-like correlations, in addition to fewer  $\text{Fe}^{3+}$  in the regions between surfboards. Both of these effects combine to reduce the inter-surfboard interactions leading to a reduced  $T_g$ . An accurate quantitative description of the behavior of  $T_g$  will require the determination of the inter-surfboard distance and other microscopic details whose investigation we leave for future studies.

We noted already that the behavior of the magnetic susceptibility and the glass transition temperature follow the trend  $d\chi(T_g)/T_g < 0$  that has been shown [4] to exist in all strongly GF magnets where  $T_g$  is modified by vacancy density. This trend can be re-expressed as the growth of the glass-transition temperature with *decreasing* vacancy density towards a finite value in the limit of zero vacancies. This finite temperature,  $T^*$ , has been called the ‘hidden energy scale’ [4] because it has not been addressed in microscopic theories of GF systems. This energy scale cannot be approached closely in  $(\text{Fe}_{(1-p)}\text{Ga}_p)_2\text{TiO}_5$  due to the different valence states of Fe and Ti, but extrapolates to  $T^* \sim 100$  K, a value far higher than seen in other strongly GF systems where  $5\text{K} < T^* < 20\text{K}$ . This difference may be due to (1) the very large  $\theta_w$  found for  $\text{Fe}_2\text{TiO}_5$  and (2) the difference between the freezing degrees of freedom. In  $\text{Fe}_2\text{TiO}_5$  these are fairly large objects, compared to an atomic spin, and their moment is induced. In the other GF systems, these are quasispins, or, the region around a vacancy and their moment is the distortion in the local spin arrangement caused by this vacancy. Despite these differences, it is reasonable to discuss  $(\text{Fe}_{(1-p)}\text{Ga}_p)_2\text{TiO}_5$  in the same framework as the other strongly GF systems since it exhibits the characteristic behavior  $d\chi(T_g)/dT_g < 0$ .

## 5. Summary

In summary, we have measured  $\chi(T)$ ,  $C(T)$ , and total neutron scattering in single crystals of  $(\text{Fe}_{(1-p)}\text{Ga}_p)_2\text{TiO}_5$ , for  $p > 0$ . We find that  $d\chi(T_g)/T_g < 0$  as the SG  $T_g$  is made to decrease with increasing  $p$ , similar to behavior seen in other GF magnets. The model proposed to explain the unusual anisotropy of the freezing anomaly at  $T_g$  for  $p = 0$  is validated for  $p = 0.20$ , in which correlated regions, albeit smaller than seen for  $p = 0$ , are observed with a concomitant reduction in  $T_g$ .

## Data availability statement

All data that support the findings of this study are included within the article (and any supplementary files).

## Acknowledgments

We thank A Henderson for assistance on materials related to but not included in this study. Work at UCSC (P L, A R) was supported by the U.S. Department of Energy Grant DE-SC0017862. Work at Argonne National Laboratory (Y L, D P, H Z, E K, A S, S R) included crystal growth; neutron scattering measurements, analysis, and interpretation; and high temperature susceptibility and was supported by the U.S. Department of Energy, Office of Science, Office of Basic Energy Sciences, Materials Sciences and Engineering Division. A portion of this research used resources at the Spallation Neutron Source, a DOE Office of Science User Facility operated by Oak Ridge National Laboratory. The work at FSU (J N and T S) was supported by the National Science Foundation Grant NSF DMR-1606952. Part of the work was carried out at the National High Magnetic Field Laboratory, which is supported by the National Science Foundation under Grant NSF DMR-1644779, and the State of Florida.

## ORCID iDs

Y Li  <https://orcid.org/0000-0002-0617-6096>

D Phelan  <https://orcid.org/0000-0003-3095-5580>

P G LaBarre  <https://orcid.org/0000-0001-9814-6486>

## References

- [1] Atzmony U, Gurewitz E, Melamud M, Pinto H, Shaked H, Gorodetsky G, Hermon E, Hornreich R M, Shtrikman S and Wanklyn B 1979 Anisotropic spin-glass behavior in  $\text{Fe}_2\text{TiO}_5$  *Phys. Rev. Lett.* **43** 782
- [2] LaBarre P G, Phelan D, Xin Y, Ye F, Besara T, Siegrist T, Syzranov S V, Rosenkranz S and Ramirez A P 2021 Fluctuation-induced interactions and the spin-glass transition in  $\text{Fe}_2\text{TiO}_5$  *Phys. Rev. B* **103** L220404
- [3] Ramirez A P 1991 Thermodynamic measurements on geometrically frustrated magnets *J. Appl. Phys.* **70** 5952
- [4] Syzranov S V and P A Ramirez 2022 Eminent phase in frustrated magnets: a challenge to quantum spin liquids *Nat. Commun.* **13** 2993
- [5] Note: The crystals used for this study were obtained from the Bell Labs Crystal Archive, the contents of which can be found at the NSF sponsored website: [www.crystalsamplearchive.org/](http://www.crystalsamplearchive.org/), where further details may be found. The particular crystals used in this study were characterized using x-ray diffraction, and electron energy-loss spectroscopy, details of which are found in the supplemental material
- [6] Ye F, Liu Y H, Whitfield R, Osborn R and Rosenkranz S 2018 Implementation of cross correlation for energy discrimination on the time-of-flight spectrometer CORELLI *J. Appl. Crystallogr.* **51** 315
- [7] Nagata S, Keesom P H and Harrison H R 1979 Low dc-field susceptibility of CuMn spin glass *Phys. Rev. B* **19** 1633
- [8] Cannella V and Mydosh J A 1972 Magnetic ordering in gold-iron alloys *Phys. Rev. B* **6** 4220
- [9] Larsen U 1978 Characteristic temperatures in the spin-glass AuFe *Phys. Rev. B* **18** 5014
- [10] Maletta H and Felsch W 1979 Insulating spin-glass system  $\text{Eu}_x\text{Sr}_{1-x}\text{S}$  *Phys. Rev. B* **20** 1245

- [11] Syzranov S 2022 Effect of vacancy defects on geometrically frustrated magnets *Phys. Rev. B* **106** L140202
- [12] Tholence J L, Yeshurun Y, Kjems J K and Wanklyn B 1987 Spin dynamics and low temperature properties of the anisotropic spin glass  $\text{Fe}_2\text{TiO}_5$  *J. Magn. Magn. Mater.* **54–57** 203–4
- [13] Binder K and Young A P 1986 Spin glasses: experimental facts, theoretical concepts, and open questions *Rev. Mod. Phys.* **58** 801
- [14] Ramirez A P 1994 Strongly geometrically frustrated magnets *Ann. Rev. Mater. Sci.* **24** 453
- [15] Nakatsuji S, Nambu Y, Tonomura H, Sakai O, Jonas S, Broholm C, Tsunetsugu H, Qiu Y M and Maeno Y 2005 Spin disorder on a triangular lattice *Science* **309** 1697
- [16] Fichtl R, Tsurkan V, Lunkenheimer P, Hemberger J, Fritsch V, von Nidda H A K, Scheidt E W and Loidl A 2005 Orbital freezing and orbital glass state in  $\text{FeCr}_2\text{S}_4$  *Phys. Rev. Lett.* **94** 027601
- [17] Silverstein H J et al 2014 Liquidlike correlations in single-crystalline  $\text{Y}_2\text{Mo}_2\text{O}_7$ : an unconventional spin glass *Phys. Rev. B* **89** 054433
- [18] Garratt S J and Chalker J T 2020 Goldstone modes in the emergent gauge fields of a frustrated magnet *Phys. Rev. B* **101** 024413
- [19] Anderson P W, Halperin B I and Varma C M 1972 Anomalous low-temperature thermal properties of glasses and spin glasses *Phil. Mag.* **25** 1
- [20] Hermele M, Fisher M P A and Balents L 2004 Pyrochlore photons: the  $U(1)$  spin liquid in a  $S=1/2$  three-dimensional frustrated magnet *Phys. Rev. B* **69** 064404
- [21] Savary L and Balents L 2012 Coulombic quantum liquids in spin-1/2 pyrochlores *Phys. Rev. Lett.* **108** 037202
- [22] Savary L and Balents L 2016 Quantum spin liquids: a review *Rep. Prog. Phys.* **80** 016502
- [23] Pace S D, Morampudi S C, Moessner R and Laumann C R 2021 Emergent fine structure constant of quantum spin ice is large *Phys. Rev. Lett.* **127** 117205
- [24] Benton O, Sikora O and Shannon N 2012 Seeing the light: experimental signatures of emergent electromagnetism in a quantum spin ice *Phys. Rev. B* **86** 075154
- [25] Syzranov S V, Yevtushenko O M and Efetov K B 2012 Fermionic and bosonic ac conductivities at strong disorder *Phys. Rev. B* **86** 241102
- [26] Isakov S V, Gregor K, Moessner R and Sondhi S L 2004 Dipolar spin correlations in classical pyrochlore magnets *Phys. Rev. Lett.* **93** 167204
- [27] Henley C L 2005 Power-law spin correlations in pyrochlore antiferromagnets *Phys. Rev. B* **71** 014424
- [28] Henley C L 2010 The “Coulomb phase” in frustrated systems *Annu. Rev. Condens. Matter Phys.* **1** 179
- [29] Sen A, Damle K and Moessner R 2011 Fractional spin textures in the frustrated magnet  $\text{SrCr}_9\text{pGa}_{12-9\text{p}}\text{O}_{19}$  *Phys. Rev. Lett.* **106** 127203
- [30] LaForge A D, Pulido S H, Cava R J, Chan B C and Ramirez A P 2013 Quasispin glass in a geometrically frustrated magnet *Phys. Rev. Lett.* **110** 017203